Aerospace Systems (2021) 4:345–352
https://doi.org/10.1007/s42401-021-00087-w

ORIGINAL PAPER

Terminal sliding mode velocity control of the electro-hydraulic actuator with lumped uncertainty

Qing Guo[1,2] · Zhenlei Chen[1,2] · Yao Yan[1,2] · Dan Jiang[3]

Received: 14 November 2020 / Revised: 30 January 2021 / Accepted: 23 February 2021 / Published online: 3 May 2021

Abstract

A terminal sliding mode control (TSMC) strategy is used in the velocity control of electro-hydraulic actuator (EHA) to improve the output response performance. Based on the terminal sliding mode technique, a disturbance observer is designed to estimate the lumped uncertainty of EHA including hydraulic parametric uncertainty and unknown external load. Different from asymptotic convergence controller, the TSMC guarantees the system state error and observer estimation error converge to zero in a finite time. The effectiveness of the proposed controller is verified by simulation results with comparisons the other controllers.

Keywords Electro-hydraulic actuator · Terminal sliding mode control · Disturbance observer · Lumped uncertainty

1 Introduction

Electro-hydraulic actuators (EHAs) are widely applied in mechanical engineering as they have power density and large load capacity, which have been used in fatigue test device [1], wheel loader [2], exoskeleton [3], and shaking tables [4]. However, there exist lumped uncertain disturbances in the EHA including hydraulic parametric uncertainties and the external load, which are unknown constant or time-varying. These uncertainties may degrade the dynamic performance of the EHA. Thus, many novel controllers have been developed such as parametric adaptive controllers [5–8], robust controllers [9–12], RBFNN controller [13], geometric controller [14], output regulation controller [15], backstepping controller with the high-gain disturbance observer [16], adaptive robust controllers [17–19], and robust controller with the extended state observer [20,21].

The aforementioned controllers used in EHAs only achieve the asymptotic convergence of the output responses. However, to the authors' best knowledge, the finite-time stability [22] of EHAs has not be addressed yet. Recently, the finite-time stabilization control has been employed in manipulator motion control [23] and strict-feedback control plant [24]. Yu et al. [25] proposed a fast terminal sliding mode control (TSMC) for SISO nonlinear systems and adopted the TSMC in robotic manipulator to achieve faster and higher precision tracking performance [26]. Chen et al. [27] used the terminal sliding mode technique in both the controller design of SISO nonlinear system and the disturbance observer design. Sun et al. [28] investigated a finite-time adaptive stabilization strategy for a class of high-order uncertain nonlinear systems. Liu [29] proposed a finite-time H_∞ controller of uncertain robotic manipulator to improve the response and the performance of the output tracking. Then He et al. [30,31] proposed an adaptive NN control to estimate the unknown modelling uncertainty and environmental dis-

This work was supported by the National Natural Science Foundation of China (no. 51775089, no. 12072068, no. 11872147), and Sichuan Science and Technology Program (no. 2020YFG0137, no. 2018JY0565).

✉ Qing Guo
guoqinguestc@uestc.edu.cn

Zhenlei Chen
zhenlei_chen@std.uestc.edu.cn

Yao Yan
y.yan@uestc.edu.cn

Dan Jiang
jdan2002@uestc.edu.cn

[1] School of Aeronautics and Astronautics, University of Electronic Science and Technology of China, Chengdu 611731, China

[2] Aircraft Swarm Intelligent Sensing and Cooperative Control Key Laboratory of Sichuan Province, Chengdu 611731, China

[3] School of Mechanical and Electrical Engineering, University of Electronic Science and Technology of China, Chengdu 611731, China

turbance. In addition, Shao et al. [32,33] also adopted many advanced control methods in quadrotors UAV to handle parametric uncertainty and external disturbance. Therefore, for many motion plants with unknown uncertainties and disturbances, these finite-time convergence controllers can be used in the industrial practice to obtain the fast and high-precision performance.

Thanks to the research development of finite-time convergent control, the study is supplied valuable intention. The main contributions of the proposed approach are given by

(i) A terminal sliding mode control is tried in the velocity feedback control of EHS to improve the fast and high-precision tracking performance. Different from [27], the hydraulic parametric uncertainties integrated with unknown external load are considered as the mismatched uncertain disturbance in the EHS model, which are extended by a disturbance observer with terminal sliding mode effect.
(ii) The effectiveness of the proposed controller is verified by comparative simulation results with the other two controllers.

2 Plant description

The EHA is a typical double-rod actuator, which is composed of a servo valve, a symmetrical cylinder, a fixed displacement pump with a servo motor and a relief valve as shown in Fig. 1. The pump is driven by the motor and outputs the supply pressure p_s. The pressure threshold of the relief valve is set as p_s. As the spool position of the servo valve $x_v > 0$, the hydraulic oil passes the servo valve and enters the left chamber. The forward channel flow Q_L and the cylinder load pressure p_L are controlled by x_v. The right chamber is connected to the return channel and the return pressure is p_r. On the other hand, the right chamber is connected to the forward channel where the load flow and pressure Q_L, p_L are controlled by the servo valve when $x_v < 0$. The channel flow is cut off as $x_v = 0$ where the load pressure can be steadily maintained.

First, the servo model is given by [34]

$$x_v = K_{sv} u, \tag{1}$$

where K_{sv} and u are the gain and the control voltage of the servo valve, respectively.

Second, the load flow Q_L is related to the cylinder load pressure p_L as follows [35]:

$$Q_L = C_d w x_v \sqrt{(p_s - \mathrm{sgn}(x_v) p_L)/\rho}, \tag{2}$$

where C_d is the discharge coefficient, w is the area gradient of the servo valve spool, ρ is the density of the hydraulic oil.

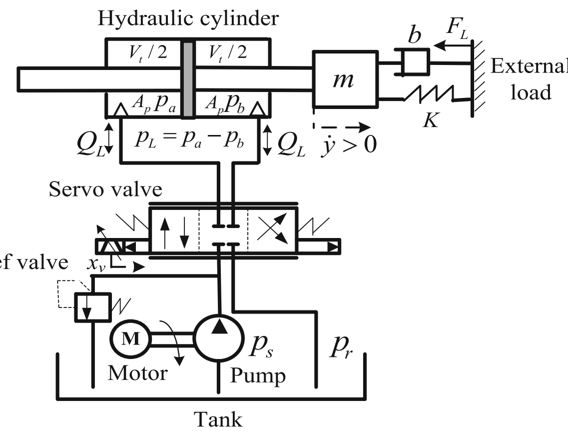

Fig. 1 The control mechanism of double-rod EHA

According to the flow conservation law, the hydraulic pressure behavior for a compressible fluid volumes, i.e., the flow-pressure continuous model, is given by [9]

$$Q_L = A_p \dot{y} + C_{tl} p_L + V_t \dot{p}_L / 4\beta_e, \tag{3}$$

where $\dot{y}$ is the piston velocity, C_{tl} is the coefficient of the total leakage of the cylinder, β_e is the effective bulk modulus, A_p is the annulus area of the cylinder chamber, V_t is the half-volume of cylinder.

Then the mechanical dynamic equation can be described as [36]

$$m\ddot{y} = p_L A_p - b\dot{y} - F_L(t), \tag{4}$$

where m is the load mass, b is the viscous damping coefficient of the hydraulic oil, F_L is the external load on the hydraulic actuator.

From (1) to (4), if we define $X = [x_1, x_2]^T = [\dot{y}, A_p p_L]^T$, then the state space model of the electro-hydraulic velocity control system is given by

$$\begin{cases} \dot{x}_1 = \dfrac{1}{m}(-bx_1 + x_2 - F_L) \\ \dot{x}_2 = -\dfrac{4\beta_e A_p^2}{V_t} x_1 - \dfrac{4\beta_e A_p C_{tl}}{V_t} x_2 \\ \qquad + \dfrac{4\beta_e C_d w K_{sv} A_p}{V_t \sqrt{\rho}} \sqrt{p_s - \mathrm{sgn}(u) x_2 / A_p} u \end{cases}. \tag{5}$$

The external load disturbance $F_L(t)$ is unknown [37]. However, $F_L(t)$ is often assumed to be bounded in practice. The two states x_1 and x_2 can be measured by the pressure transducer and the encoder.

Generally, the hydraulic parameters C_d, ρ, w, K, b, β_e, C_{tl} are often perturbed by different hydraulic physical characteristics [8]. Hence, these parameters can be written as $C_d = \bar{C}_d + \Delta C_d$, $\rho = \bar{\rho} + \Delta\rho$, $w = \bar{w} + \Delta w$, $b = \bar{b} + \Delta b$,

$\beta_e = \bar{\beta}_e + \Delta\beta_e$, $C_{tl} = \bar{C}_{tl} + \Delta C_{tl}$, where $\bar{*}$ is the nominal value of $*$, $\Delta*$ is the parametric uncertainty.

Then, in view of parametric uncertainties, the model in (5) can be formulated as

$$\begin{cases} \dot{x}_1 = f_1(x_1) + g_1 x_2 + d_{L1} \\ \dot{x}_2 = f_2(x_1, x_2) + g_2(x_2, u)u + d_{L2} \end{cases}, \tag{6}$$

where

$$\begin{aligned} f_1 &= -\frac{\bar{b}x_1}{m}, \quad g_1 = \frac{1}{m}, \quad d_{L1} = \frac{-F_L - \Delta b x_1}{m} \\ f_2 &= -\frac{4\bar{\beta}_e A_p^2}{V_t} x_1 - \frac{4\bar{\beta}_e A_p \bar{C}_{tl}}{V_t} x_2 \\ g_2 &= \frac{4\bar{\beta}_e \bar{C}_d \bar{w} K_{sv} A_p}{V_t \sqrt{\bar{\rho}}} \sqrt{p_s - \mathrm{sgn}(u) x_2 / A_p} \\ d_{L2} &= \Delta f_2(x_1, x_2, \Delta\beta_e, \Delta C_{tl}) \\ &\quad + \Delta g_2(x_1, x_2, \Delta C_d, \Delta w, \Delta\rho) \end{aligned}. \tag{7}$$

Remark 1 The two lumped uncertain disturbances d_{L1} and d_{L2} are caused by parametric uncertainties and unknown external load.

Assumption 1 These two disturbances $d_{Li}(i = 1, 2)$ are bounded by $|d_{Li}| \le d_{Li\,\max}$, where $d_{Li\,\max}$ is a known value for $i = 1, 2$.

3 Terminal sliding mode control

3.1 Preliminaries

Lemma 1 [26,38] *If a positive definite Lyapunov function $V(x, t) \ge 0$ yields that*

$$\dot{V}(x, t) + \mu V(x, t) + \delta V^{\alpha}(x, t) \le 0, \forall t \ge t_0, \tag{8}$$

then $V(t)$ converges to the equilibrium point x_0 in finite time t_f bounded by

$$t_f \le t_0 + \frac{1}{\mu(1+\alpha)} \ln \frac{\mu V^{1-\alpha}(t_0) + \delta}{\delta}, \tag{9}$$

where $\mu, \delta > 0$, $0 < \alpha < 1$ are positive constants, t_0 is the initial time with respect to x_0.

Definition 1 [25] For the low-triangle strict-feedback nonlinear system

$$\begin{cases} \dot{x}_1 = f(x_1) + g_1(x_1)x_2 \\ \cdots\cdots \\ \dot{x}_i = f(\bar{x}_i) + g_i(\bar{x}_i)x_{i+1} \\ \cdots\cdots \\ \dot{x}_n = f(\bar{x}_n) + g_n(\bar{x}_n)u \end{cases}, \tag{10}$$

where $\bar{x}_i = [x_1, \ldots, x_i]$, the terminal sliding mode surface has n orders form, which can be derived by the recursive procedure given by

$$\begin{cases} s_1 = x_1 - y_d \\ s_2 = \dot{s}_1 + \mu_1 s_1 + \delta_1 s_1^{p_1/q_1} \\ \vdots \\ s_n = \dot{s}_{n-1} + \mu_{n-1} s_{n-1} + \delta_{n-1} s_{n-1}^{p_{n-1}/q_{n-1}} \end{cases}, \tag{11}$$

where $s_i(i = 1, \ldots, n)$ are the n orders terminal sliding mode surfaces, $p_i < q_i(i = 1, \ldots, n-1)$ are positive odd integers, y_d is the desirable output.

3.2 TSM disturbance observer

The sliding mode surfaces of two lumped uncertain disturbances $d_{Li}(i = 1, 2)$ are designed as follows:

$$s_i = v_i - x_i, \quad i = 1, 2, \tag{12}$$

where $v_i(i = 1, 2)$ are two disturbance observer variables.

To guarantee the finite time convergence to the disturbances, $v_i(i = 1, 2)$ are designed to satisfy the following forms:

$$\begin{cases} \dot{v}_1 = -k_{d1}s_1 - D_1\mathrm{sgn}(s_1) - \varepsilon_1 s_1^{p_0/q_0} + f_1 + g_1 x_2 \\ \dot{v}_2 = -k_{d2}s_2 - D_2\mathrm{sgn}(s_2) - \varepsilon_2 s_2^{p_1/q_1} + f_2 + g_2 u \end{cases}, \tag{13}$$

where $k_{di}(i = 1, 2)$ are the observer gains, $\varepsilon_i, D_i(i = 1, 2) > 0$ are positive constants, $p_i < q_i(i = 0, 1)$ are positive odd integers.

Then the estimates of the two disturbances are written as

$$\begin{cases} \hat{d}_{L1} = -k_{d1}s_1 - D_1\mathrm{sgn}(s_1) - \varepsilon_1 s_1^{p_0/q_0} \\ \hat{d}_{L2} = -k_{d2}s_2 - D_2\mathrm{sgn}(s_2) - \varepsilon_2 s_2^{p_1/q_1} \end{cases}. \tag{14}$$

Lemma 2 [27] *Consider the disturbance observer (13) and the velocity control system (5) under Assumption 1. If the positive constants $D_i > d_{Li\,\max}(i = 1, 2)$, then disturbance observer is convergent in finite time.*

Proof To begin with, the following Lyapunov functions are considered:

$$V_i = \frac{1}{2}s_i^2, \quad i = 1, 2. \tag{15}$$

Then the time derivative of V_i takes the form

$$\begin{aligned}\dot{V}_i &= s_i \dot{s}_i = s_i(\dot{v}_i - \dot{x}_i) \\ &= s_i(-k_{\mathrm{d}i} s_i - D_i \operatorname{sgn}(s_i) - \varepsilon_i s_i^{p_{i-1}/q_{i-1}} + f_i \\ &\quad + g_i x_{i+1} - f_i - g_i x_{i+1} - d_{\mathrm{L}i}) \\ &\le -k_{\mathrm{d}i} s_i^2 - D_i s_i \operatorname{sgn}(s_i) - \varepsilon_i s_i^{p_{i-1}+q_{i-1}/q_{i-1}} \\ &\quad + |s_i|\,|d_{\mathrm{L}i}|\end{aligned} \quad . \tag{16}$$

Due to $D_i > d_{\mathrm{L}i\,\max}(i = 1, 2)$, and by Assumption 1, (16) is rewritten as

$$\begin{aligned}\dot{V}_i &\le -k_{\mathrm{d}i} s_i^2 - D_i\,|s_i| - \varepsilon_i s_i^{p_{i-1}+q_{i-1}/q_{i-1}} + |s_i|\,|d_{\mathrm{L}i}| \\ &\le -k_{\mathrm{d}i} s_i^2 - \varepsilon_i s_i^{p_{i-1}+q_{i-1}/q_{i-1}} \\ &\le -k_{\mathrm{d}i} V_i - 2^{(p_{i-1}+q_{i-1})/2q_{i-1}} \varepsilon_i V_i^{(p_{i-1}+q_{i-1})/2q_{i-1}}\end{aligned} \quad , \tag{17}$$

for $i = 1, 2$. For the convenience of derivation, we assume the virtual variable $x_3 = u$.

According to Lemma 1, two sliding mode surfaces $s_i(i = 1, 2)$ converge to the origin in a finite time. Meanwhile, from (14), the observation errors take the form

$$\begin{aligned}\tilde{d}_{\mathrm{L}i} &= \hat{d}_{\mathrm{L}i} - d_{\mathrm{L}i} \\ &= -k_{\mathrm{d}i} s_i - D_i \operatorname{sgn}(s_i) - \varepsilon_i s_i^{p_{i-1}/q_{i-1}} \\ &\quad + f_i + g_i x_{i+1} - \dot{x}_i \\ &= \dot{v}_i - \dot{x}_i = \dot{s}_i\end{aligned} \quad , \tag{18}$$

for $i = 1, 2$.

Since $s_i(i = 1, 2)$ are finite-time stable at the origin, $\dot{s}_i(i = 1, 2)$ approach zero in finite time. Hence, the two disturbance observer errors $\tilde{d}_{\mathrm{L}i}(i = 1, 2)$ converges to zero in finite time.

3.3 Terminal sliding mode controller design

Assumption 2 [39] It is assumed that $y_\mathrm{d}(t)$ and its ith order derivatives $y_\mathrm{d}^{(i)}(t), i = 1, 2, 3$ satisfy $|y_\mathrm{d}(t)| \le Y_0 < k_{\mathrm{c}1}$ and $\left|y_\mathrm{d}^{(i)}(t)\right| \le Y_i$, where $Y_i(i = 0, 1, 2, 3)$ are positive constants.

To achieve the finite-time velocity control of the EHA, two sliding mode surfaces are designed as follows:

$$\begin{cases} \xi_1 = x_1 - \dot{y}_\mathrm{d} + s_1 \\ \xi_2 = \dot{\xi}_1 + \mu_1 \xi_1 + \delta_1 \xi_1^{p_1/q_1} + g_1 s_2 - \dfrac{\bar{b}}{m} s_1 \end{cases} . \tag{19}$$

Substituting the time derivative of ξ_1 into ξ_2, we have

$$\begin{aligned}\xi_2 &= \dot{x}_1 - \ddot{y}_\mathrm{d} + \dot{s}_1 + \mu_1 \xi_1 + \delta_1 \xi_1^{p_1/q_1} + g_1 s_2 - \frac{\bar{b}}{m} s_1 \\ &= f_1 + g_1 x_2 + d_{\mathrm{L}1} - \ddot{y}_\mathrm{d} + \tilde{d}_{\mathrm{L}1} \\ &\quad + \mu_1 \xi_1 + \delta_1 \xi_1^{p_1/q_1} + g_1 s_2 - \frac{\bar{b}}{m} s_1 \\ &= f_1 + g_1 x_2 + \hat{d}_\mathrm{L} - \ddot{y}_\mathrm{d} + \mu_1 \xi_1 \\ &\quad + \delta_1 \xi_1^{p_1/q_1} + g_1 s_2 - \frac{\bar{b}}{m} s_1\end{aligned} \quad . \tag{20}$$

Then the time derivative of ξ_2 takes the form

$$\begin{aligned}\dot{\xi}_2 &= -\frac{\bar{b}}{m}(f_1 + g_1 x_2 + d_{\mathrm{L}1}) + g_1(f_2 + g_2 u + d_{\mathrm{L}2}) \\ &\quad + \dot{\hat{d}}_{\mathrm{L}1} - \dddot{y}_\mathrm{d} + \mu_1 \dot{\xi}_1 + \delta_1 \frac{\mathrm{d}(\xi_1^{p_1/q_1})}{\mathrm{d}t} + g_1 \dot{s}_2 - \frac{\bar{b}}{m} \dot{s}_1 \\ &= -\frac{\bar{b}}{m}(f_1 + g_1 x_2 + \hat{d}_{\mathrm{L}1}) + g_1(f_2 + g_2 u + \hat{d}_{\mathrm{L}2}) \\ &\quad + \dot{\hat{d}}_{\mathrm{L}1} - \dddot{y}_\mathrm{d} + \mu_1 \dot{\xi}_1 + \delta_1 \frac{\mathrm{d}(\xi_1^{p_1/q_1})}{\mathrm{d}t}\end{aligned} \quad . \tag{21}$$

Lemma 3 *Consider the two sliding mode surfaces (19) and the velocity control system (5). Based on the disturbance observer (13), if the terminal sliding mode controller (TSMC) is designed by*

$$\begin{aligned}u = -\frac{1}{g_1 g_2}\Bigg[&- \frac{b}{m}(f_1 + g_1 x_2 + \hat{d}_{\mathrm{L}1}) + g_1(f_2 + \hat{d}_{\mathrm{L}2}) \\ &+ \dot{\hat{d}}_{\mathrm{L}1} - \dddot{y}_\mathrm{d} + \mu_1 \dot{\xi}_1 + \delta_1 \frac{\mathrm{d}(s_1^{p_1/q_1})}{\mathrm{d}t} + \mu_2 \xi_2 + \delta_2 \xi_2^{p_2/q_2} \Bigg]\end{aligned} , \tag{22}$$

then all closed-loop signals of the EHA are stable in the finite time t_f and the EHA velocity satisfies $|x_1(t) - \dot{y}_\mathrm{d}(t)| \to 0, t \to t_f$ for any given velocity command y_d.

Proof Consider the following candidate Lyapunov function

$$V_3 = \frac{1}{2}\xi_2^2. \tag{23}$$

Substituting (21) into the time derivative of V_3, we can obtain that

$$\dot{V}_3 = \xi_2\Big[-\frac{\bar{b}}{m}(f_1 + g_1 x_2 + \hat{d}_{L1}) + g_1(f_2 + g_2 u + \hat{d}_{L2}) + \dot{\hat{d}}_{L1} - \dddot{y}_d + \mu_1 \dot{\xi}_1 + \delta_1 \frac{d(\xi_1^{p_1/q_1})}{dt} \Big] \quad (24)$$

Then consider the controller u in (22), and we have

$$\begin{aligned}\dot{V}_3 &\le -\mu_2 \xi_2^2 - \delta_2 \xi_2^{p_2+q_2/q_2} \\ &\le -2\mu_2 V_3 - 2^{(p_2+q_2)/2q_2} \delta_2 V_3^{(p_2+q_2)/2q_2}\end{aligned} \quad (25)$$

According to Lemma 1, the sliding mode variable ξ_2 is finite-time stable. Furthermore, from (19), ξ_2 a function of ξ_1, s_1 and s_2. Since the two observer sliding mode variables $s_i (i = 1, 2)$ converge to zero in a finite time by Lemma 2, ξ_1 is also convergent in a finite time. Due to $\dot{y}_d$ is bound by Assumption 2 and $s_1 \to 0, t \to t_f$, x_1 is also bounded from ξ_1. Hence, ν_1 is bounded from the definition of s_1 in (12). Then $\dot{\nu}_1$ is bounded which, in turn, derives x_2 converge to zero in finite-time using (13). By (19), since $\xi_2 \to 0, t \to t_f$, $\xi_1 \to 0$ and $|x_1(t) - \dot{y}_d(t)| \to 0$ as $t \to t_f$.

The block diagram of the terminal sliding mode control scheme is shown in this Fig. 2. The whole closed-loop system includes two sliding mode surfaces $s_i, \xi_i (i = 1, 2)$ for the disturbance observe $\hat{d}_{Li} (i = 1, 2)$ and the TSMC u. According to the TSM stable condition (8), u is designed to guarantee the EHA (1) is finite-time stable. The block diagram of the terminal sliding mode control scheme

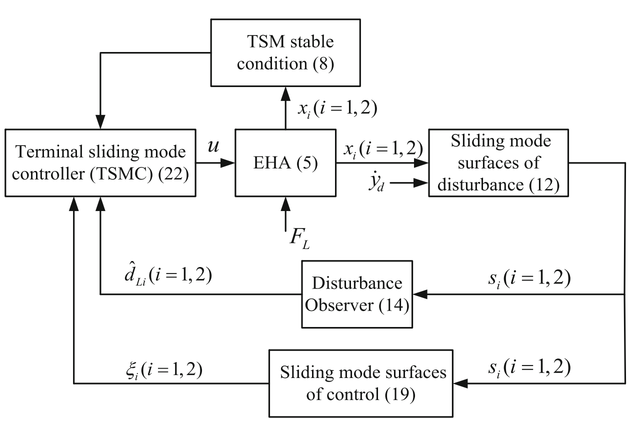

Fig. 2 The block diagram of the terminal sliding mode control scheme

4 Simulation results

To verify the TSMC, some nominal hydraulic parameters of the EHA are given by $\bar{C}_d = 0.62$, $\Delta C_d = 0.1\bar{C}_d$, $\bar{w} = 0.024$ m, $\Delta w = 0.1\bar{w}$, $\bar{C}_{tl} = 2.5 \times 10^{-11}$ m^3/(s Pa), $\Delta C_{tl} = 0.3\bar{C}_{tl}$, $\bar{\beta}_e = 7000$ bar, $\Delta\beta_e = 0.1\bar{\beta}_e$, $\bar{\rho} = 850$ kg/m^3, $\Delta\rho = 0.15\bar{\rho}$, $\bar{b} = 50$ Ns/m, $\Delta b = 0.2\bar{b}$, $K_{sv} = 5 \times 10^{-4}$ m/V, $T_{sv} = 10$ ms, $x_{vmax} = 5$ mm, $L_{max} = 78$ mm, $p_s = 40$ bar, $p_r = 2$ bar, $A_p = 4.91$ cm^2, $V_t = 8.74 \times 10^{-5}$ m^3. The manipulator load mass is $m = 6$ kg. The disturbance observer parameters are $k_{d1} = k_{d2} = 1000$, $D_1 = 30$, $D_2 = 100$, $\varepsilon_1 = 100$, $\varepsilon_2 = 10$, $p_0 = p_1 = 5$, $q_0 = q_1 = 7$. The TSM controller parameters $\mu_1 = 10^4$, $\mu_2 = 100$, $\delta_1 = \delta_2 = 1$, $p_2 = 5$, $q_2 = 9$ are set. The cylinder velocity demands are chosen as $\dot{y}_d = 30\sin(0.5\pi t)$ mm/s and $\dot{y}_d = \text{square}(\pm 30)$ mm/s, respectively. The corresponding external load of the EHA is

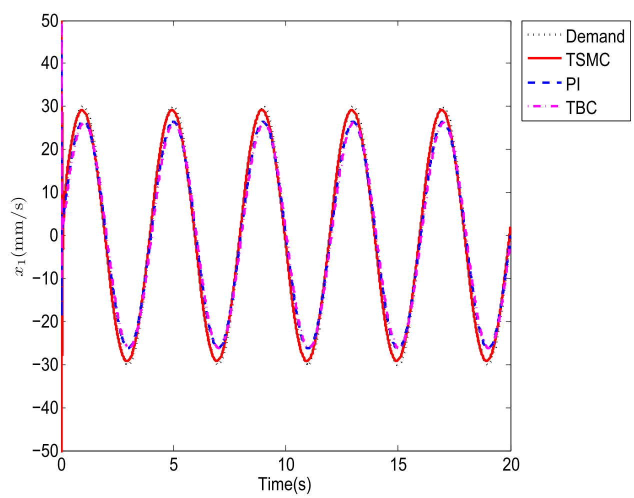

Fig. 3 The cylinder velocity response of three controllers in simulation for the demand $\dot{y}_d = 30\sin(0.5\pi t)$ mm/s

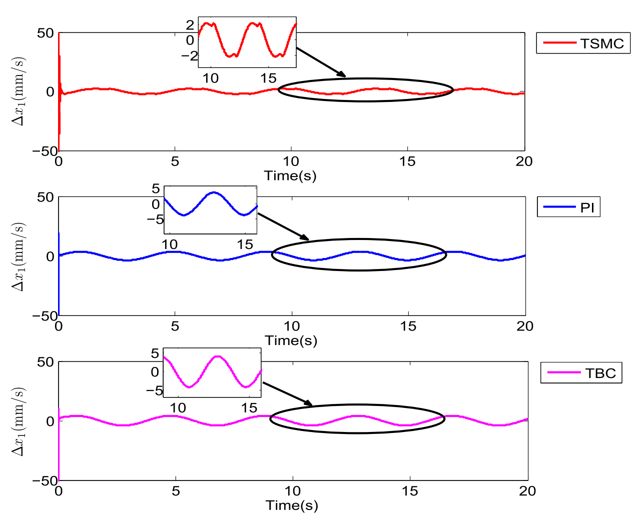

Fig. 4 The tracking errors of the cylinder velocity in simulation for the demand $\dot{y}_d = 30\sin(0.5\pi t)$ mm/s

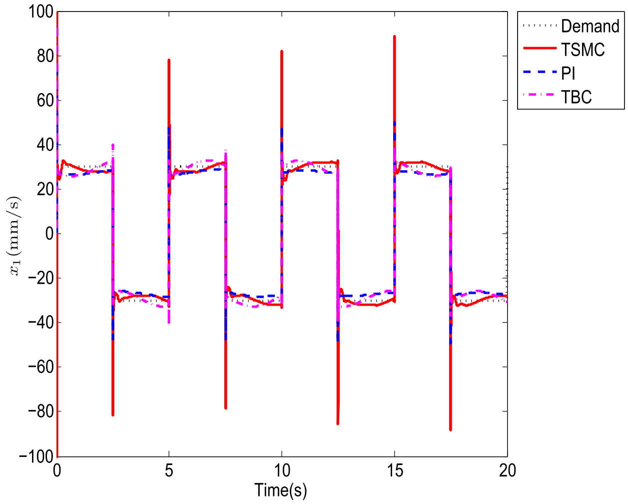

Fig. 5 The cylinder velocity response of three controllers in simulation for the demand $\dot{y}_d$ = square (±30) mm/s

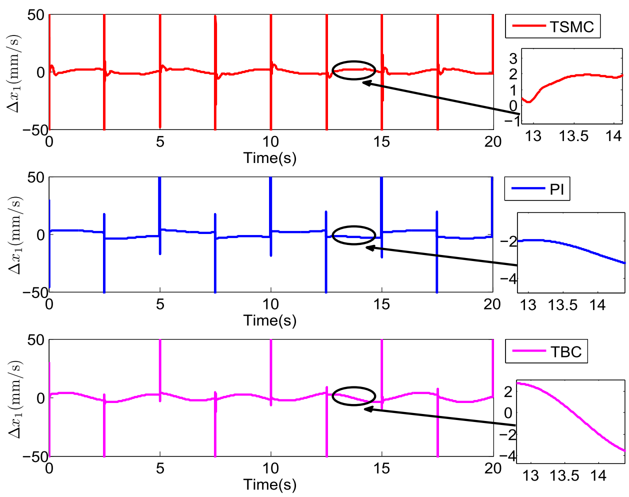

Fig. 6 The tracking errors of the cylinder velocity in simulation for the demand $\dot{y}_d$ = square (±30) mm/s

assumed to be $F_L(t) = 100\sin(0.5\pi t)$ N and $F_L(t) = 100$ N. To make a comparison, the other two controllers are also applied for the EHA:

1) PI controller $u = k_p(\dot{y}_d - x_1) + k_i\int(\dot{y}_d - x_1)\mathrm{d}t$, where the control gains $k_p = 100$ and $k_i = 10$ are chosen to guarantee the fast response of EHA.
2) the traditional backstepping controller (TBC), given by

$$\begin{cases} \zeta_1 = (-k_1 z_1 - f_1 + \ddot{y}_d)/g_1 \\ u = (-k_2 z_2 - f_2 - g_1 z_1 + \dot{\zeta}_1)/g_2 \end{cases}, \tag{26}$$

where $z_1 = x_1 - \dot{y}_d$ and $z_2 = x_2 - \zeta_1$, ζ_1 is the virtual control variable, $f_1 = \bar{b}x_1/m$, $g_1 = 1/m$, $f_2 = -4\bar{\beta}_e A_p^2 x_1/V_t - 4\bar{\beta}_e \bar{C}_{tl} A_p x_2/V_t$, $g_2 = 4\bar{\beta}_e \bar{C}_d \bar{w} K_{sv} A_p \sqrt{p_s - \mathrm{sgn}(\eta u) x_2/A_p} / (V_t\sqrt{\bar{\rho}})$, $k_1 = 2000$, $k_2 = 1000$.

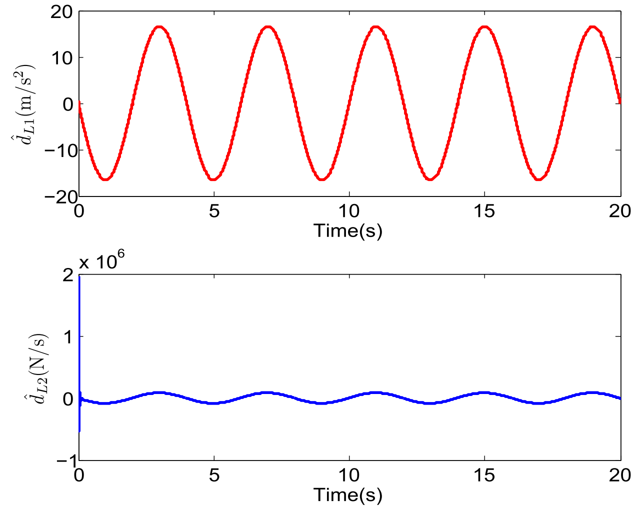

Fig. 7 The two disturbance estimations by the TSM controller in simulation for the demand $\dot{y}_d = 30\sin(0.5\pi t)$ mm/s

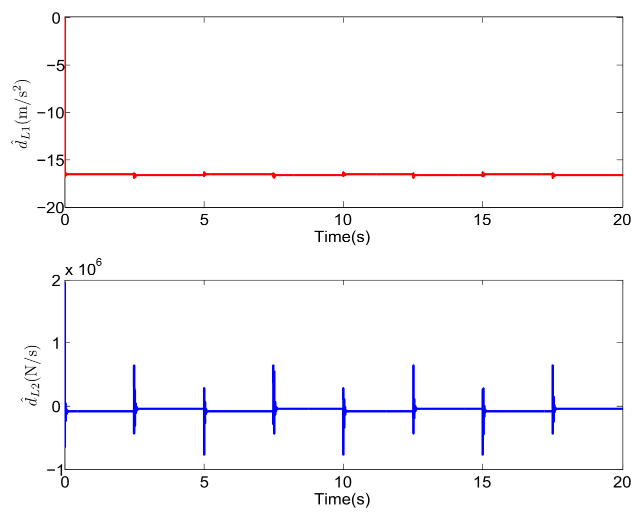

Fig. 8 The two disturbance estimations by the TSM controller in simulation for the demand $\dot{y}_d$ = square (±30) mm/s

The simulation results under the two types of demands are shown in Figs. 3, 4, 5, 6, 7, 8, 9 and 10. All the three controllers guarantee that the cylinder velocity can track the two types of demands with performance. However, the tracking performance subject to the TSMC is better than the PI and backstepping controllers in both scenarios, as shown in Figs. 4 and 6. Meanwhile, the disturbance estimates generated by the proposed observer are shown in Figs. 7 and 8, which are employed in the TSM controller (22). By a further inspection, these disturbance estimates are consistent with the dynamics of the external load F_L and the model functions f_2, g_2. The two sliding mode surfaces and the corresponding TSM controller output of two demands are shown in Figs. 9 and 10,

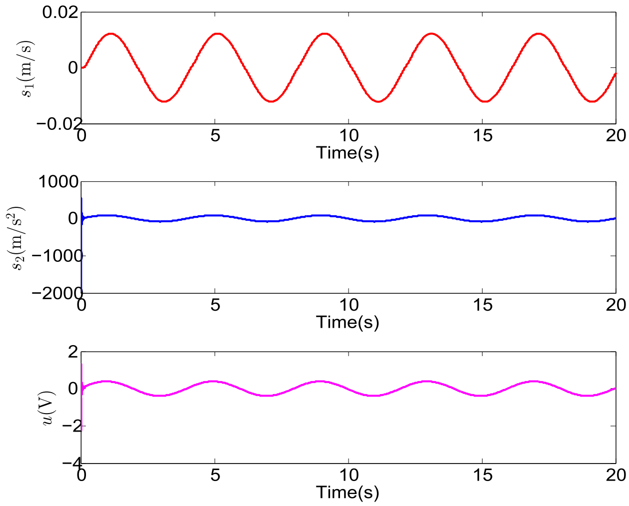

Fig. 9 The two sliding mode surfaces and the TSM controller output in simulation for the demand $\dot{y}_{\mathrm{d}} = 30\sin(0.5\pi t)$ mm/s

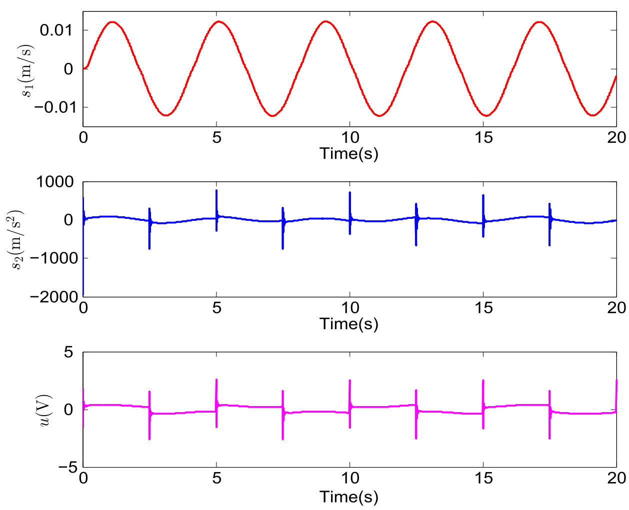

Fig. 10 The two sliding mode surfaces and the TSM controller output in simulation for the demand $\dot{y}_{\mathrm{d}} =$ square (± 30) mm/s

which guarantee the electrohydraulic system stable by the proposed TSM controller.

5 Conclusions

In this study, a terminal sliding mode control (TSMC) strategy is used in the electro-hydraulic actuator under lumped uncertain disturbance. Based on the strict-feedback nonlinear model of the electro-hydraulic velocity control loop, the proposed controller is designed based on the sliding mode control and the. By proposing a new disturbance TSM observer, the lumped uncertain disturbances are estimated and compensated in the TSMC design. The simulation results with comparisons demonstrate that the proposed control strategy achieves faster responses and better tracking performance. In the future work, the experimental bench of the manipulator driving by EHA will verify the proposed control scheme.

References

1. Zhao J, Wang J, Wang S (2013) Fractional order control to the electro-hydraulic system in insulator fatigue test device. Mechatronics 23(7):828–839
2. Fales R, Kelkar A (2009) Robust control design for a wheel loader using H_∞ and feedback linearization based methods. ISA Trans 48(3):313–320
3. Yang Y, Ma L, Huang D (2017) Development and repetitive learning control of lower limb exoskeleton driven by electro-hydraulic actuators. IEEE Trans Ind Electron 64(5):4169–4178
4. Shen G, Li X, Zhu Z, Tang Y, Zhu W, Liu S (2017) Acceleration tracking control combining adaptive control and off-line compensators for six-degree-of-freedom electro-hydraulic shaking tables. ISA Trans 70:322–337
5. Yao B, Bu F, Reedy J, Chiu GTC (2000) Adaptive robust motion control of single-rod hydraulic actuators theory and experiments. IEEE/ASME Trans Mechatron 5(1):79–91
6. Kaddissi C, Kenné JP, Saad M (2011) Indirect adaptive control of an electrohydraulic servo system based on nonlinear backstepping. IEEE/ASME Trans Mechatron 16(6):1171–1177
7. Guo Q, Zuo Z, Ding Z (2020) Parametric adaptive control of single-rod electrohydraulic system with block-strict-feedback model. Automatica 113:108807
8. Yao J, Deng W, Sun W (2017) Precision motion control for electro-hydraulic servo systems with noise alleviation: a desired compensation adaptive approach. IEEE/ASME Trans Mechatron 22(4):1859–1868
9. Milić V, Željko Šitum M, Essert M (2010) Robust H_∞ position control synthesis of an electro-hydraulic servo system. ISA Trans 49(4):535–542
10. Guo Q, Yu T, Jiang D (2015) Robust H_∞ positional control of 2-dof robotic arm driven by electro-hydraulic servo system. ISA Trans 59:55–64
11. Shen W, Pang Y, Jiang J (2018) Robust controller design of the integrated direct drive volume control architecture for steering systems. ISA Trans 78:116–129
12. Chen Z, Yao B, Wang Q (2015) μ-synthesis-based adaptive robust control of linear motor driven stages with high-frequency dynamics: a case study. IEEE/ASME Trans Mechatron 20(3):1482–1490
13. Guo Q, Chen Z (2021) Neural adaptive control of single-rod electrohydraulic system with lumped uncertainty. Mech Syst Signal Proc 146:106869
14. Ursu I, Toader A, Halanay A, Balea S (2013) New stabilization and tracking control laws for electrohydraulic servomechanisms. Eur J Control 19(1):65–80
15. Song X, Wang Y, Sun Z (2014) Robust stabilizer design for linear time-varying internal model based output regulation and its application to an electro hydraulic system. Automatica 50(4):1128–1134
16. Won D, Kim W, Shin D, Chung CC (2015) High-gain disturbance observer-based backstepping control with output tracking error constraint for electro-hydraulic systems. IEEE Trans Control Syst Technol 23(2):787–795
17. Chen Z, Yao B, Wang Q (2013) Adaptive robust precision motion control of linear motors with integrated compensation of nonlinearities and bearing flexible modes. IEEE Trans Ind Informat 9(2):965–973

18. Yao J, Jiao Z, Ma D (2015) A practical nonlinear adaptive control of hydraulic servomechanisms with periodic-like disturbances. IEEE/ASME Trans Mechatron 20(6):2752–2760
19. Sun W, Gao H, Kaynak O (2015) Vibration isolation for active suspensions with performance constraints and actuator saturation. IEEE/ASME Trans Mechatron 20(2):675–683
20. Yao J, Jiao Z, Ma D (2014) Extended-state-observer-based output feedback nonlinear robust control of hydraulic systems with backstepping. IEEE Trans Ind Electron 24(6):993–1015
21. Li S, Wei J, Guo K, Zhu W (2017) Nonlinear robust prediction control of hybrid active-passive heave compensator with extended disturbance observer. IEEE Trans Ind Electron 64(8):6684–6694
22. Bhat SP, Bernstein DS (1997) Finite-time stability of homogeneous systems. In: Proceedings of 1997 American control conference. pp 2513–2514
23. Hong Y, Xu Y, Huang J (2002) Finite-time control for robot manipulators. Syst Control Lett 46(4):243–253
24. Huang X, Lin W, Yang B (2005) Global finite-time stabilization of a class of uncertain nonlinear systems. Automatica 41(5):881–888
25. Yu X, Man Z (2002) Fast terminal sliding-mode control design for nonlinear dynamical systems. IEEE Trans Circuits Syst I Fundam Theory 49(2):261–264
26. Yu S, Yu X, Shirinzadeh B, Man Z (2005) Continuous finite-time control for robotic manipulators with terminal sliding mode. Automatica 41(11):1957–1964
27. Chen M, Wu Q, Cui R (2013) Terminal sliding mode tracking control for a class of siso uncertain nonlinear systems. ISA Trans 52:198–206
28. Sun Z, Xue L, Zhang K (2015) A new approach to finite-time adaptive stabilization of high-order uncertain nonlinear system. Automatica 58:60–66
29. Liu H, Tian X, Wang G, Zhang T (2016) Finite-time H_∞ control for highprecision tracking in robotic manipulators using backstepping control. IEEE Trans Ind Electron 63(9):5501–5513
30. He W, David AO, Yin Z, Sun C (2016) Neural network control of a robotic manipulator with input deadzone and output constraint. IEEE Trans Syst Man Cybern A Syst 46(6):759–770
31. He W, Yan Z, Sun C, Chen Y (2017) Adaptive neural network control of a flapping wing micro aerial vehicle with disturbance observer. IEEE Trans Cybern 47(10):3452–3465
32. Shao X, Liu J, Wang H (2018) Robust back-stepping output feedback trajectory tracking for quadrotors via extended state observer and sigmoid tracking differentiator. Mech Syst Signal Process 104:631–647
33. Shao X, Liu J, Cao H, Shen C, Wang H (2018) Robust dynamic surface trajectory tracking control for a quadrotor uav via extended state observer. Int J Robust Nonlinear 104:631–647
34. Kim W, Shin D, Won D, Chung CC (2013) Disturbance-observer-based position tracking controller in the presence of biased sinusoidal disturbance for electrohydraulic actuators. IEEE Trans Control Syst Technol 21(6):2290–2298
35. Guo Q, Yin J, Yu T, Jiang D (2017) Saturated adaptive control of an electrohydraulic actuator with parametric uncertainty and load disturbance. IEEE Trans Ind Electron 64(10):7930–7941
36. Guan C, Pan S (2008) Nonlinear adaptive robust control of single-rod electro-hydraulic actuator with unknown nonlinear parameters. IEEE Trans Control Syst Technol 16(3):434–445
37. Guo Q, Zhang Y, Celler BG, Su SW (2016) Backstepping control of electro-hydraulic system based on extended-state-observer with plant dynamics largely unknown. IEEE Trans Ind Electron 63(11):6909–6920
38. Man Z, Yu X (1997) Terminal sliding mode control of mimo linear systems. IEEE Trans Circuits Syst I Fundam Theory 44(11):1060–1065
39. Tee KP, Ge SS, Tay EH (2009) Barrier lyapunov functions for the control of output-constrained nonlinear systems. Automatica 45(1):918–927